

A Study on Thermal Properties of Composite Metal Foams for Applications in Tank Cars Carrying Hazardous Materials



Afsaneh Rabiei, Nigel Amofo-Yeboah, Evan Huseboe, and Claire Scemama

Abstract Each year, millions of tons of hazardous materials are shipped through tank cars on railroads. Accidents involving these tank cars can create punctures that release these hazardous materials into the surrounding area, resulting in potential fire and even explosions, human fatalities, and substantial damage to the environment. Despite all enhancements to mitigate the consequences of such accidents, there is still an immediate need for novel material with superior puncture and fire resistance with lower weight than the current carbon-steel in use, to improve the safety and efficacy of tank cars carrying hazardous materials (HAZMAT). Composite metal foam (CMF) is a novel class of light-weight material made of closely packed metallic hollow spheres with a surrounding metallic matrix. In this study, the latest developments on evaluating the performance of composite metal foam against extreme heat through both experimental and analytical approaches will be reported and compared to those properties of the base bulk steel materials in use.

Keywords Composite metal foam · Thermal conductivity · Specific heat capacity · Coefficient of thermal expansion · Thermal diffusivity

Introduction

In a growing global and industrialized economy, there is an increasing need for transportation of a variety of industrial and hazardous materials (HAZMAT). Such transportations have a high susceptibility of creating catastrophic damages to the environment and individuals, if not handled carefully. The United States Department of Transportation (DOT) has played an important role in ensuring that standards are met to avert any catastrophic occurrences during transportation of HAZMAT. Such efforts gave rise to the development of the DOT-117 tank car with the DOT117-R standards, which emphasizes on the thermal protection of these tank cars [1]. These standards require that the thermal resistance within the tank car should be sufficient

A. Rabiei (✉) · N. Amofo-Yeboah · E. Huseboe · C. Scemama
Department of Mechanical and Aerospace Engineering, North Carolina State University, Raleigh,
NC 27695, USA
e-mail: arabiei@ncsu.edu

to prevent any laden release except through pressure release devices when subjected to a 100 min pool fire at 871 ± 55.6 °C and a 30 min torch fire at 1204 ± 55.6 °C [2]. Owing to steel's load-carrying capacity, the maximum fail/pass temperature for these tests is set at 427 °C [2]. This is due to the fact that at 427 °C carbon-steel (the main material used in the structure of tank cars) still maintains 60% of its yield strength after which the strength drops rapidly.

The novel steel composite metal foam (CMF) developed at North Carolina State University has shown superior mechanical properties as compared to the conventional bulk steel [3–6] making it a superior candidate for protecting against potential puncture in case of derailment and accidents. Preliminary studies in assessing the performance of composite metal foam (CMF) in simulated pool fire [3, 7] and small-scale torch fire [4] environments indicated promising performances in application of CMF in the structure of tank cars. In prior studies, thermal properties of composite metal foams (CMFs) have been reported between room temperature and 600 °C [5]. In order to validate the application of CMF in the structure of tank cars, full-scale torch fire testing must be conducted. As the full-scale torch fire experiment requires expensive torch fire testing on very large panels, a computation modeling approach can be the first step to predict the required specifications of composite metal foam (CMF) to withstand such torch fire exposures. In order to implement CMF properties in the torch fire model, it is necessary to evaluate its properties at elevated temperatures up to the torch fire conditions. The focus of this study will be to investigate thermal conductivity, specific heat capacity, and coefficient of thermal expansion of composite metal foam (CMF) from room temperature to 1000 °C.

Materials and Methods

Steel-Steel Composite Metal Foam (S-S CMF) samples were manufactured using powder metallurgy technique [6]. Hollow stainless steel spheres with nominal diameters of 2 and 4 mm with wall thicknesses of 100 and 200 μm , respectively, are shaken into a random-loose packing arrangement within a steel mold and surrounded with a 316 L stainless steel powder. The mold is then heated within a vacuum hot press up to 1200 °C for sintering followed by passively cooling under high vacuum to room temperature. Detailed information regarding the manufacturing process of steel-steel composite metal foam (S-S CMF) using powder metallurgy technique can be found in previous studies [6, 8, 9]. Stainless steel spheres used for processing the steel-steel composite metal foam (S-S CMF) panel were manufactured by Hollomet GmbH located in Dresden, Germany. The 316 L stainless steel powder used as the matrix material to surround hollow steel spheres was obtained from North American Höganäs with an average particle size of 44 μm . Steel-steel composite metal foam (S-S CMF) was manufactured in a variety of dimensions and sizes to be used for various thermal tests planned in this study. The following section focuses on the preparation of the samples for each set of thermal property measurements.

Table 1 Dimensions and densities of samples used for CTE measurements

Sample name	Sample length (mm)	Sample diameter (mm)	Sample density (g/cc)
4 mm SS-CMF 1	25.15	9.66	2.77
4 mm SS-CMF 2	25.12	9.51	2.83
4 mm SS-CMF 3	25.12	9.54	2.76
2 mm SS-CMF 1	25.99	9.53	2.63
2 mm SS-CMF 2	24.95	9.61	3.12
Solid stainless steel	25.51	9.00	7.89

Coefficient of Thermal Expansion

Coefficient of thermal expansion (CTE) measurements were conducted on cylindrical samples of steel-steel composite metal foam (S-S CMF). The samples were cut by electrical discharge machining (EDM) and then hand sanded to ensure that each surface of the sample was reflective and blemish free. To remove any leftover debris, the samples were cleaned with acetone in an ultrasonic cleaner and dried to remove any possible moisture present within the porosities of the material. A cylindrical solid 304 stainless steel sample was prepared to be used as a control sample for this test. This sample was also cut using the EDM process and then sanded and cleaned in the same fashion. An Adventurer OHAUS (M/N AR3130) scale was used to measure the mass to an accuracy of ± 1 mg and a lab caliper with an accuracy of ± 0.01 mm was used for physical dimensions. The dimensions and densities of various samples used in coefficient of thermal expansion (CTE) measurements can be found in Table 1. A digital image of one of the samples used to evaluate the coefficient of thermal expansion is shown in Fig. 1.

Thermal Conductivity and Specific Heat Capacity

Four steel-steel composite metal foam (S-S CMF) cylindrical samples with nominal dimensions of 25.4 mm diameter (actual diameters measuring $25.1 \text{ mm} \pm 0.2 \text{ mm}$) and height of 6 mm (actual height $5.85 \pm 0.15 \text{ mm}$) were cut from S-S CMF rods on a Buehler Isomet 4000 linear precision saw. Due to the constraints imposed by the thermal diffusivity measuring device (maximum thickness of 6 mm), only 2 mm sphere steel-steel composite metal foam (S-S CMF) samples were used to evaluate the thermal conductivity of S-S CMF samples. This is due to the fact that cutting

Fig. 1 4 mm steel-steel composite metal foam (S-S CMF) prepared for coefficient of thermal expansion measurements

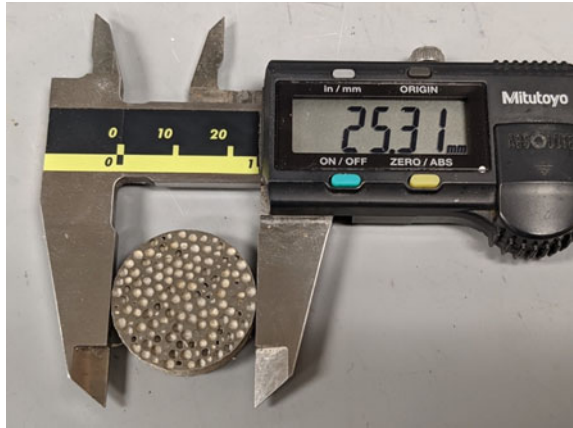


composite metal foam (CMF) samples made with larger sphere diameters of 4 mm or 6 mm into 6 mm thick samples may not result in meaningful repeatable data. The cross sections of all samples were then polished on a Buehler workstation using a progression of 180, 240, 320, 600, and 800 grit SiC sandpaper at a wheel speed of 50 RPM. Before proceeding to the next grit size of sandpaper, samples were cleaned in a water bath in an ultrasonic cleaning machine to prevent cross contamination. In the final stage, samples were cleaned with acetone in an ultrasonic cleaner to remove any leftover debris and moisture and then dried. An Adventurer OHAUS (M/N AR3130) scale was used to measure the mass to an accuracy of ± 1 mg and a lab caliper with an accuracy of ± 0.01 mm was used for physical dimensions. Table 2 shows the dimensions and densities of the samples that were prepared for evaluating the thermal conductivity and thermal diffusivity measurements of steel-steel composite metal foam (S-S CMF) samples from room temperature up to 1000 °C. A digital image of one of the samples that was used to evaluate the thermal conductivity of the steel-steel composite metal foam (S-S CMF) is shown in Fig. 2.

Table 2 Steel-steel composite metal foam (S-S CMF) samples used for thermal conductivity and diffusivity measurements

Name	Diameter (mm)	Thickness (mm)	Mass (g)	Density (g/cc)
Sample 1	25.3	5.96	7.87	2.63
Sample 2	25.0	5.72	7.20	2.55
Sample 3	25.0	5.91	7.77	2.68
Sample 4	24.8	5.93	7.40	2.58

Fig. 2 Steel-steel composite metal foam [S-S CMF] sample prepared for thermal conductivity and diffusivity measurements



Experimental Procedures

Coefficient of Thermal Expansion

The coefficient of thermal expansion (CTE) of the 2 and 4 mm sphere steel-steel composite metal foam [S-S CMF] samples was evaluated using the ASTM E228 standard [10]. This method uses a push rod dilatometer to measure the linear thermal expansion of the samples. The dilatometer used in this experimental process is an Orton Dilatometer Model 2010 STD (120 VAC 50/60 Hz), which has a furnace chamber capable of heating up to 1000 °C. For each measurement, the sample holder was thoroughly cleaned using ethanol and compressed air, to remove any debris that may have built up during the prior runs. This was done to prevent any slippage during thermal expansion that could affect the accuracy of results. After cleaning the chamber, the sample was carefully placed in the sample holder with the push rod firmly touching the end of the sample. The Linear Variable Differential Transformer (LVDT) was initialized to 0.100 using a built-in micrometer gauge. Sample length was inputted into the software and testing parameters set. The tests were run in air from room temperature to 1000 °C at a heating rate of 3 °C/min.

Figure 3 shows the Orton Dilatometer used for the CTE measurements with one of the samples set on it.

Thermal Conductivity, Thermal Diffusivity, and Specific Heat Capacity

The thermal conductivity is calculated from the thermal diffusivity measurement using the flash method, per ASTM E1461 [11]. The testing was conducted at the TA

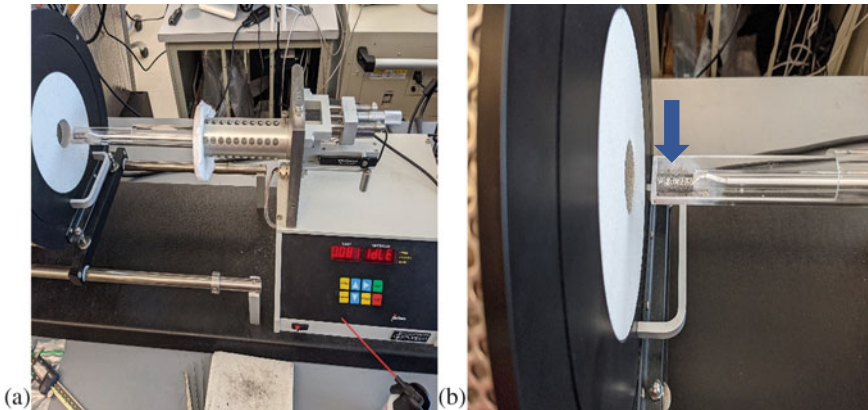


Fig. 3 **a** Orton dilatometer used for CTE measurements. **b** Sample in place for testing (marked by blue arrow)

Instruments Thermophysical Contract Testing Services department using a Discovery Laser Flash DLF-1200 which is a compact benchtop instrument for the measurement of thermal diffusivity, thermal conductivity, and specific heat of materials from room temperature to 1200 °C. The test method uses a 300–400 μs flash from a Class 1 Nd: Glass laser to heat the sample with up to 17 J of energy from one side, while monitoring the other side with a 16-bit, high-speed infrared (IR) detector. The response time is measured to calculate thermal diffusivity using Parker's relationship [12]. The instrument is rated to be accurate to $\pm 2.3\%$ for thermal diffusivity and $\pm 4\%$ for thermal conductivity. The instrument is also rated to be repeatable to $\pm 2.0\%$ for thermal diffusivity and $\pm 3.5\%$ for thermal conductivity [12].

To evaluate the thermal conductivity, each sample's density was measured, along with its thermal diffusivity. Density was calculated using measured sample dimensions and mass as reported in Table 2.

Testing procedure starts with a calibration run. The DLF-1200, shown in Fig. 4, was calibrated with a thermo-graphite reference sample within 5% of reference values, and calibration run was repeated for each sample to verify each test's accuracy. Prior to the test, colloidal graphite was sprayed on both sides of each sample to maximize absorptivity and emissivity. The composite metal foam (CMF) sample was placed in a two-sample holder, the other sample being the reference thermo-graphite. The samples were heated at 10 °C/min to the set temperature and then held at the set temperature. Once the sample reached equilibrium at the set temperature, the Nd laser flash was pulsed on the bottom of the sample. The top of the sample was monitored by the IR detector, which recorded temperature data. The temperature data was processed through the TA Instrument's software, which accounts for energy losses by the standard Clark & Taylor model [13]. This single flash procedure was repeated three times per temperature point to strike an average. The three samples were tested at the following temperature points: Room Temperature, 200, 400, 600, 700, 827, 900, and 1000 °C. The specific heat in J/gC was then calculated using the

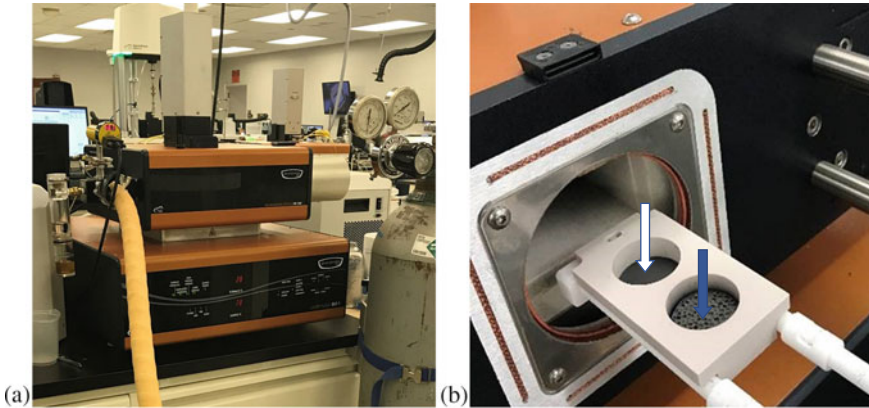


Fig. 4 **a** DLF-1200 Testing Instrument used to measure composite metal foam’s. (CMF’s) thermal diffusivity and conductivity. **b** Reference thermo-graphite (marked by white arrow) and composite metal foam (CMF) sample (marked by blue arrow) right before furnace insertion

equation:

$$\lambda = \alpha * Cp * \rho \tag{1}$$

in which λ is the Thermal Conductivity, α is the Thermal Diffusivity or the rate of temperature spread through a material (m^2/s)—direct measurement from the laser flash experiment based on Parker’s Relationship (explained above), Cp is the Specific Heat as per Mills et al. [14], and ρ is the Density—inputed value based on reference measurements and data reported in Table 2.

It is notable that given the composition of the S-S CMF being the same as 316 L SS, and the fact that the specific heat of all metal foams is reported to be the same as their parent materials [15], we use the specific heat of solid 316 L stainless steel [16] in this equation.

Results and Discussion

Coefficient of Thermal Expansion

Table 3 shows CTE results obtained from 100 to 1000 °C for tested 304 stainless steels as compared to literature values. Measured CTE values range from 16.09 to 19.55E-06, which indicates an agreement with referenced literature values. As a control run, this suggests a suitable degree of accuracy for CTE values measured using this approach.

Table 4 shows the average CTE measurements obtained from various steel-steel

Table 3 Measured 304 stainless steel CTE values compared to literature values

Nominal temperature (°C)	Measured 304 stainless steel CTE ($\times 10^{-6}$)	Literature CTE ($\times 10^{-6}$) [17]
100	16.09	16.02
200	16.68	17.1
300	17.02	17.64
400	17.54	18
500	17.91	18.36
600	18.27	18.72
700	18.71	19.26
800	19.22	19.44
900	19.46	–
1000	19.55	–

Table 4 Coefficient of thermal expansion (CTE) measurements of all 2 and 4 mm steel-steel composite metal foam [S-S CMF] samples compared with 316 L stainless steel (from literature)

Temperature (°C)	Average CTE of S-S CMF with 2 mm sphere (E-06)	Average CTE of S-S CMF with 4 mm sphere (E-06)	316L CTE (E-06) [18]	%Difference between 316 L steel and 2 mm sphere S-S CMF	%Difference between 316 L steel and 4 mm sphere S-S CMF
100	16.45 \pm 1.24	17.05 \pm 0.69	15.39	6.66	10.21
200	16.74 \pm 0.13	16.77 \pm 0.72	16.21	3.19	3.40
300	16.81 \pm 0.37	16.83 \pm 0.32	16.86	0.30	0.18
400	16.95 \pm 0.44	17.13 \pm 0.37	17.37	2.45	1.39
500	17.38 \pm 0.38	17.37 \pm 0.34	17.78	2.28	2.31
600	17.86 \pm 0.37	17.86 \pm 0.31	18.12	1.47	1.45
700	18.38 \pm 0.53	18.49 \pm 0.35	18.43	0.30	0.34
800	18.68 \pm 0.66	19.07 \pm 0.36	18.72	0.24	1.87
900	18.82 \pm 0.64	20.07 \pm 0.42	18.99	0.90	5.55
1000	19.00 \pm 0.82	21.18 \pm 0.45	19.27	1.41	9.44

composite metal foam [S-S CMF] samples as compared to literature data for 316L stainless steel [18]. As can be seen, the coefficient of thermal expansion (CTE) of S-S CMF is within the same range as that of the CTE of its parent material with less than 10% difference only. All data indicate a good level of repeatability with an average standard deviation of 0.43E-06. It also shows that there is not much of a big difference between the CTE of the steel-steel composite metal foam (S-S CMF) made with 2 and 4 mm hollow spheres. This is due to the fact that the sphere wall thickness to the outer diameter ratio in both composite metal foam [CMF] type samples is kept

constant, and as such, the % of metal and air content in the material is maintained the same in both sets of the samples. In comparison to bulk 316 L stainless steel, the S-S CMFs made from 316 L stainless steel show comparable CTE values. It indicates that the air inside the porosities of CMF does not have a major impact on the coefficient of thermal expansion of S-S CMF. Similar behavior has been reported in CTE of other metal foam compared to their parent materials [15]. However, since CMF consists of both matrix and porosities, it was essential to confirm such behavior at various temperatures prior to any modeling efforts.

Thermal Conductivity, Thermal Diffusivity, and Specific Heat Capacity

Table 5 gives a summary of thermal properties of bulk 316L stainless steel and S-S CMF at various temperatures. As can be seen, the thermal conductivity of steel-steel composite metal foam (S-S CMF) is about 5–6 times lower than that of its parent material (316 L). The measured diffusivity of steel-steel composite metal foam (S-S CMF) shows diffusivity increasing from 2.3 to 3.8 mm²/s with rising temperature whilst that of its parent bulk steel ranges from 3.74 to 5.95 mm²/s. This also puts the ratio of diffusivity of steel-steel composite metal foam (S-S CMF) to bulk stainless steel to be approximately 1:2.

Thermal diffusivity is the measure of the rate of heat transfer from the hot to the cold side of a material, which is measured as $\alpha = \frac{k}{\rho c_p}$ as outlined in prior sections.

Table 5 Thermal properties of bulk steel and the steel-steel composite metal foam [S-S CMF]

Temperature (°C)	Thermal properties of solid 316 L solid stainless steel			Thermal properties of 316 L S-S CMF	
	Diffusivity (mm ² /s) [16]	Specific heat (J/g C) [16]	Conductivity (W/m C) [16]	Experimental diffusivity (mm ² /s)	Experimental conductivity (W/m C)
26	3.6	0.47	13.4	2.317 ± 0.045	2.920 ± 0.05
100	4.0	0.49	15.5	–	–
196	4.3	0.52	17.4	2.573 ± 0.087	3.570 ± 0.10
300	4.6	0.54	19.4	–	–
398	5.0	0.56	21.3	2.880 ± 0.090	4.230 ± 0.10
500	5.3	0.57	23.4	–	–
598	5.4	0.59	24.3	3.203 ± 0.054	4.96 ± 0.10
699	5.5	0.60	25.1	3.373 ± 0.119	5.35 ± 0.18
823	5.7	0.63	27.3	3.653 ± 0.141	5.92 ± 0.25
896	5.8	0.64	27.6	3.707 ± 0.181	6.14 ± 0.26
996	5.9	0.66	28.3	3.773 ± 0.218	6.39 ± 0.32

Since the density of S-S CMF was measured to be an average of 2.6 g/cc (almost 1/3rd of its parent 316 L density of 8) and specific heat capacity used is the same as that of its parent material, it can be seen from the equation that the density, thermal conductivity, and diffusivity are impacted by the volume fractions of air in the composite metal foam (CMF). This is better understood in an attempt made to analytically determine the thermal conductivity of the steel-steel composite metal foam (S-S CMF).

Considering the CMF as a composite material made of air and metal components, with the air component being uniformly dispersed and arbitrarily placed in a metallic matrix, the effective thermal conductivity (K_{eff}) was estimated using the simple rule of mixture as seen in Eq. (2) [5]:

$$k_{eff} = \frac{k_m \phi_m + k_a \phi_a \frac{3k_m}{(2k_m + k_a)} + k_{sw} \phi_{sw} \frac{3k_m}{(2k_m + k_a)}}{\phi_m + \phi_a \frac{3k_m}{(2k_m + k_a)} + \phi_{sw} \frac{3k_m}{(2k_m + k_a)}} \quad (2)$$

where k_m and k_{sw} represent the thermal conductivities of the matrix and sphere wall where $k_m = k_{sw}$ (both made of 316L stainless steel) and k_a represents the thermal conductivities of air inside the foam. The variables ϕ_m , ϕ_{sw} , and ϕ_a are the respective volume fractions of the matrix, sphere wall, and air inside (both inside the hollow spheres and within the micro-porosities of the matrix). These volume fractions were calculated for the CMF samples based on the densities used in this current study as 21%, 12%, and 67%, respectively. Data obtained after analytical calculations are also presented in Table 6.

Comparing the analytical thermal conductivity reported in Table 6 and the experimental thermal conductivities of the composite metal foam (CMF) samples, it is clear that the analytical results are comparable to those of experimental data with a percentage difference ranging from 13–25%. This difference can be related to the distribution of numerous small air pockets in the structure of the CMF where the convection and radiation are more dominating than conduction, and those were not accounted for in this simple analytical evaluation. A simple illustration of the heat path through a composite metal foam (CMF) is shown in Fig. 5. As 59 volume percent of the composite metal foam (CMF) is made of spheres and 41% is the matrix, and the air content inside the cavity of spheres is about 70–80% of the total volume of each sphere (depending on the wall thickness to sphere radius ratio), the air content inside the spheres is estimated to be about 41–47%, respectively. This air content creates a major thermal barrier in CMF. Moreover, from the 41% matrix in the structure of CMF, about 45–47% is air in its micro-porosities that makes up about 18.5–19.3% of air in the matrix, respectively (depending on the compaction of the matrix powder). The large air contents in the cavity of spheres can only allow heat convection and radiation with no conduction, while the air content in the micro-porosities of the matrix (manufacturing using powder metallurgy) will also lower the conductivity of the matrix by disturbing the heat path. The predicted analytical conductivity did not consider the interferences within the heat path through the many porosities both in the matrix and spheres and many interfaces of air and metal. In fact, there is about

Table 6 Comparison between the analytical and experimental thermal conductivities of the steel-steel composite metal foam (S-S CMF) and the conductivities of the main components of S-S CMF (air and 316 L)

Temperature (°C)	Thermal conductivity of 316 L matrix and sphere wall (W/m C)	Thermal conductivity of air (W/m C) [19]	Experimental thermal conductivity of S-S CMF (W/m C)	Analytical conductivity of S-S CMF (W/m C)	%Difference between the analytical and experimental thermal conductivity of S-S CMF
25	13.4	0.025	2.92	3.33	13.22
100	15.5	0.031	–	3.86	–
200	17.6	0.038	3.57	4.38	20.44
300	19.4	0.044	–	4.83	–
400	21.8	0.050	4.23	5.43	24.88
500	23.4	0.056	–	5.83	–
600	24.5	0.061	4.96	6.11	20.74
700	25.1	0.066	5.35	6.26	15.69
823	27.3	0.071	5.92	6.78	13.60
900	27.9	0.076	6.14	6.96	12.53
1000	29.1	0.079	6.39	7.26	12.75

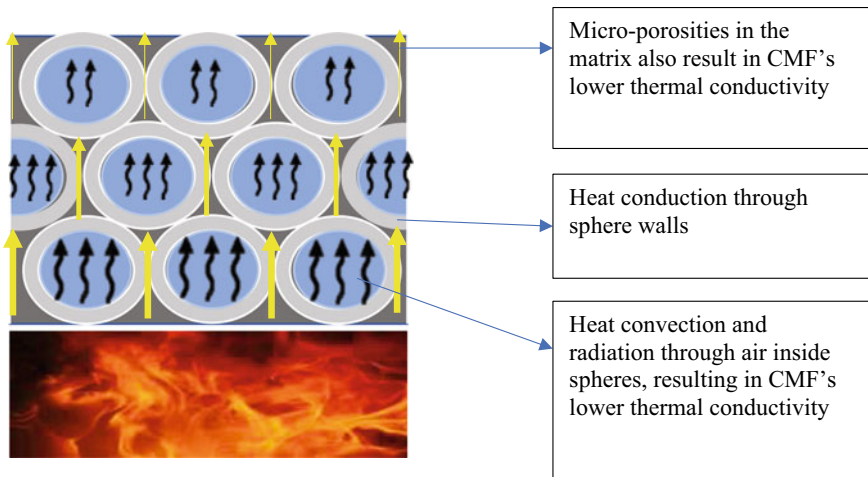


Fig. 5 An illustration of heat path through composite metal foam structure

65–70% air in structure of CMF that is distributed throughout the material (including both the air within the matrix and in the cavity of the hollow spheres) that lowers the conductivity of CMF as seen in this study. The presence of air porosities creates an insulating effect, which largely hinders the effective flow of thermal energy through the foams. The total air content in the structure of CMF depends on the sphere wall thickness and the amount of pressure applied during its manufacturing, and as such, the thermal conductivity of composite metal foam (CMF) can be tailored to each specific need.

Conclusions

Data gathered from thermal property measurements indicated that S-S CMF's thermal conductivity is about 6 times lower than that of its parent bulk steel, while its density is 1/3rd of the steel and its diffusivity is half of that of steel. These are due to the presence of high-volume fractions of air in the CMF. Data from thermal conductivity and thermal diffusivity measurements show that CMF can be tailored to the desired thermal properties based on the matrix to sphere ratios and the wall thickness of the spheres. This study also confirms the theory that CTE and specific heat capacity values of S-S CMFs are the same as those of their parent material and the sphere size has minimal effect on the thermal properties of CMF as long as the wall thickness to radius ratio is maintained constant.

Acknowledgements This research was supported by the Department of Transportation (DOT) Pipeline and Hazardous Materials Safety Administration (PHMSA) under project number # PH957-20-0075.

References

1. Thomas D (2015) Railway age. <https://www.railwayage.com/regulatory/dot-117-tank-car-rule-debuts-with-some-controversy/>
2. Cornell Law School, Legal Information Institute, open Access to Law since 1992. <https://www.law.cornell.edu/cfr/text/49/179.202-13>
3. Rabiei A, Karimpour K, Janssens M, Basu D (2020) Simulated pool fire testing and modeling of a composite metal foam. *Fire Mater* 2020:1–8
4. Rabiei A, Lattimer BY, Bearinger E (2021) Recent advances in the analysis, measurement, and properties of composite metal foams. In: TMS 2021 150th Annual meeting and exhibition supplemental proceedings, Chapter 13
5. Chen S, Marx J, Rabiei A (2016) Experimental and computational studies on the thermal behaviour and fire retardant properties of composite metal foams. *Int J Therm Sci* 106:70–79
6. Neville B, Rabiei A (2008) Composite metal foams processed through powder metallurgy. *Mater Des* (29):388–396

7. Rabiei A, Karimpour K, Basu D, Janssens M (2020) Steel-steel composite metal foam in simulated pool fire testing. *Int J Therm Sci* 153(106336)
8. Rabiei A (2015) Composite metal foam and methods of preparation thereof. Patent US9208912B2
9. Rabiei A, Garcia-Avila M (2013) Effect of various parameters on properties of composite steel foams under variety of loading rates. *Mater Sci Eng A* 564:539–547
10. E228–17, Standard Test Method for Linear Thermal Expansion of Solid Materials with a Push-Rod Dilatometer
11. ASTM E1461-13 (E1461.14396) Standard test method for thermal diffusivity by the flash method
12. Instruments T. Thermal conductivity and diffusivity. <https://www.tainstruments.com/wp-content/uploads/BROCH-ThermalConductivityDiffusivity-EN.pdf>
13. Clark III LM, Taylor RE (1975) Radiation loss in the flash method for thermal diffusivity. *J Appl Phys* 46:714
14. Mills KC, Su YLZ, Brooks RF (2004) Equations for the calculation of the thermo-physical properties of stainless steel. *ISIJ Int* 44(10):1661–1668
15. Ashby M, Evans A, Fleck N, Gibson L, Hutchinson J, Wadley H (2000) *Metal foams: a design guide*. Butterworth-Heinmann, Massachusetts
16. Mills KC (2002) Recommended values of thermophysical properties for selected commercial alloys, Cambridge CB1 6AH. Woodhead Publishing Limited, England
17. Alloys RR. Thermal expansion. <https://www.rolledalloys.com/technical-resources>
18. Shan X, Davies CM, Wangsdan T, O'Dowd NP, Nikbion KM (2009) Thermo-mechanical modelling of a single-bead-on-plate weld using the finite element method. *Int J Press Vessels Pip* 86:110–121
19. Hurley MJ SFPE handbook of fire protection engineering table A23. Fifth edn. Springer, New York. <https://doi.org/10.1007/978-1-4939-2565-0>